Electronic Supplementary Information

Enhancement of Electrochemical Performance of Zinc-Silver Batteries by a Gold Nano-Scaffold

Pritha Mondal,‡ Ajeet Kumar Rana,‡ Subham Kumar Saha, Akhila Subhakumari, Navyashree Vasudeva, Naga Phani

---

Solid State and Structural Chemistry Unit,
Indian Institute of Science,
Bangalore 560012, India.
Email: anshup@iisc.ac.in

B. Aetukuri and Anshu Pandey *

1.   Preparation of the active material (Au-Ag nanostructures)

1.1.   Materials:

Cetylammonium bromide (CTAB) from Sigma-Aldrich (≥98% pure), silver nitrate (AgNO$_3$) from Sigma-Aldrich (ACS reagent, ≥99.0% pure), sodium borohydride powder (NaBH$_4$) from Sigma-Aldrich (≥98.0% pure), chloroauric acid (HAuCl$_4$) from Sigma-Aldrich (ACS, 99.99% pure, metal basis) and iso propyl alcohol (IPA) from SDFCL (AR, ACS grade) were used as received. All the aqueous solutions have been prepared in milli-Q water to avoid any trace of metal contamination. All the aqueous solutions have been prepared in 18.2 M-Ohm milli-Q water to avoid any metal contamination.

Optimization of reaction timing: It is mentioned in the manuscript that the time of addition of the reducing agent NaBH$_4$ is crucial to attain the required size of the Ag nanoparticles (~ 1 nm). Even though there was slight variation (~ 4-5 sec) for different CTAB batches used, the addition time was always around 20 s.

The extinction spectrum of small Ag nanoparticles (~ 1 nm) is shown in Figure S1a (blue curve). The spectrum does not exhibit the characteristic localized surface plasmon resonance (LSPR) feature at around 3.1 eV. This is due to the high surface to volume ratio of the nanoparticles. As a result, there is a significant surface scattering of electrons and the plasmonic feature is damped. However, in case of large Ag nanoparticles (> 5nm) the extent of this surface scattering is decreased compared to the smaller particles, hence those large nanoparticles exhibit the LSPR feature at 3.1 eV. It was observed that when the time of addition of NaBH$_4$ was > 1 min, the Ag nanoparticles formed were large, which exhibited the LSPR feature at 3.1 eV (Fig S1a, black curve). However, these bigger Ag nanoparticles are not appropriate for inclusion into Au matrix.

Furthermore, when these large Ag nanoparticles were used to synthesize the Ag-Au nanostructures, we observed separate nucleation. This is shown in the extinction spectrum where the two types of nanoparticles exhibit two distinct resonance peaks at 2.3 eV and 3.1 eV each corresponding to Au and Ag LSPR respectively (Fig S1b, red curve). However, when there is proper incorporation of the Ag nanoparticles into the Au matrix (as shown in the TEM images in Fig 2), the extinction spectrum of these bimetallic nanostructure exhibits no plasmonic feature. Instead, the nanostructures exhibit an almost flat spectrum (Fig S1b, brown curve).

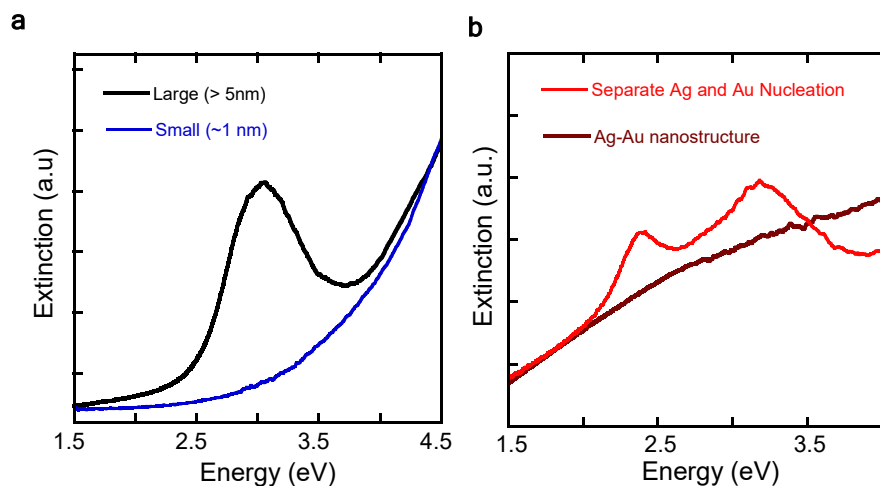The detailed synthetic procedure is given below.

Fig. S1 (a) Optical extinction spectrum of small (blue curve) and large (black curve) Ag nanoparticles. **(b)** Optical extinction spectrum of the Ag-Au nanostructures (brown curve) and separately nucleated Ag and Au nanoparticles (red curve).

1.2. Synthesis of Ag nanoparticles:

Aqueous solutions of 0.1 M CTAB (2 mL) was mixed with 0.5 mL of 10 mM $AgNO_3$. The mixture was stirred continuously for 20 s, followed by addition of 2 mL of 0.1 M freshly prepared, ice-cold, aqueous solution of $NaBH_4$ to produce a yellowish solution - (solution 1).

1.3. Synthesis of Au-Ag nanostructures:

In the first step aqueous solution of 1 mM $HAuCl_4$ was added to the silver nanoparticles (solution 1) with continuous stirring to produce a brown color solution-(solution2). Depending on the amount of Ag and Au to be maintained in the resultant nanostructures, the amount of 1 mM $HAuCl_4$ solution added was changed. The amounts used were 0.52 mL, 1.25 mL and 2.14 mL for the Ag: Au ratio of 9:1, 8:2 and 7:3 respectively.

In the second step, 3 mL of IPA was added to 5 mL of solution 2 to produce a dark brown solution. Finally, the above reaction mixture was centrifuged for 5 minutes at 4100 RCF. A dark precipitate adhered to the sides of centrifuge tube and the supernatant was discarded. The precipitate was dried under a vacuum of ~ 10 mbar.
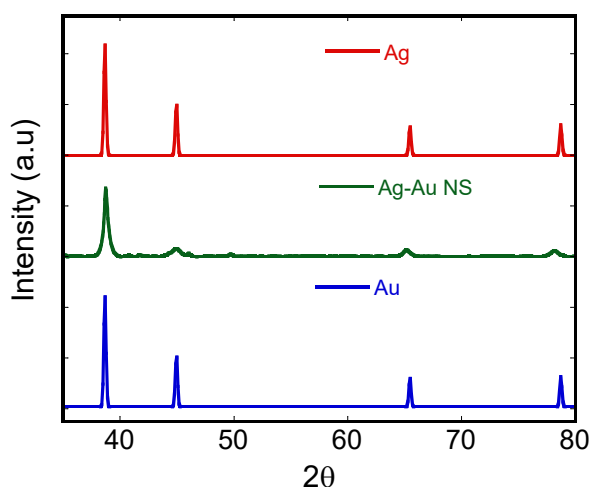

Fig. S2: Powder XRD pattern of the Ag-Au nanostructures (green) is in good agreement with the standard pattern of Au (blue) and Ag (red).

2. Preparation of the electrode for Zn-Ag battery (Au-Ag nanostructures)

2.1 Materials:

Potassium hydroxide (KOH) from SDFCL (AR grade), polytetrafluoroethylene binder (PTFE) from Sigma-Aldrich, Conductive carbon (TIMCAL Graphite and Carbon Super P) was used as received. 1 cm × 3 cm Avcarb P-50 carbon paper was used to make the electrode. Milli-Q water was used for aqueous solution preparation and other purposes to avoid any trace of unwanted metal contaminations.

2.2 Preparation of Ag – Au Electrode:

Au-Ag nanostructures (70% by wt.) were mixed with conductive carbon black (20% by wt.) and PTFE binder (10% by wt.), a minimum volume of water was added and the whole mixtures were mixed thoroughly with the help of sonicator and vortex mixture. The conductive carbon black was used to increase the conductivity and PTFE was used as a binder because it is water soluble, and it is stable in basic KOH solution. The above mixtures were sonicated for 5 minutes and then mixed with vortex mixture for 5 minutes. The above procedure was repeated for 1 hour and 15 minutes to get the slurry. Now this slurry was drop-casted on 1×3 cm Avcarb P-50 carbon paper. After that the drop-casted carbon paper was dried at 60 ℃ in a vacuum oven for 12 hours. This prepared electrode was used for all the electrochemical measurements.

2.3 Preparation of Ag Electrode:

A similar protocol as above was used for the preparation of electrode using 70 % Ag-nanoparticle, 20 % conductive carbon black and 10 % PTFE binder.

3. Electrochemical measurements:

100 mL 0.5 M KOH solution (pH = 13) was taken in a three-naked flat bottom flask. The above prepared electrode was used as a working electrode and 0.5×2 cm Zn metal foil (thickness 0.5 mm) was used as a reference and counter electrode. Both Ag – Au working electrode and Zn metal foil as reference and counter electrode were dipped in above flask containing KOH solution to assemble the Zn – Ag battery. The inert argon (Ar) gas was purged for 15 minutes during electrochemical measurements.

First Open-Circuit Potential was done for 1 hour to let the system attain equilibrium. After that cyclic voltammetry at different scan rates: 1, 5, 10, 20, 50 and 100 mV s^{-1} were performed. Two redox reactions were observed. To check the reversibility of both the redox, Cyclic Voltammetry at scan rate 50 mV s^{-1} was performed for 50 cycles. After that Galvanostatic Charge-Discharge (GCD) was performed at C-rate 1C for 35 cycles.

3.1   Comparison with literature

Ragone plot as well as table has been given below for the comparison of our work with previously published Zn-Ag battery works.

Table S1: Comparison of specific capacities of various published work with the data for Zn-Ag batteries fabricated in this work.

| Battery type	Capacity (mAh g^{-1})	Energy density (Wh kg^{-1})	Power density (W kg^{-1})	Cycle life	References
Zn-AgO	100	148	99	30	[1]
Zn-Ag$_2$O	~86	129	5.16	Primary	[2]
Zn-Ag$_2$O	45	67.5	135	Primary	[3]
Ag/paper/Zn-Ag	~56.3	85	280	5	[4]
Zn-Ag	37.3	56	56	Primary	[5]
Zn-Ag (1 redox)	55	90.5	258.6	35	This work
Zn-Ag/Au (9:1) – 1 redox	82	125	595		
Zn-Ag/Au (8:2) – 1 redox	94	141	427.3		
Zn-Ag/Au (7:3) – 1 redox	60	90	353		
Zn-Ag (2 redox)	80	131.3	227.2		
Zn-Ag/Au (9:1) – 2 redox	155	250	408.7		
Zn-Ag/Au (8:2) – 2 redox	220	354	355.7		
Zn-Ag/Au (7:3) – 2 redox	165	268.5	382.2		
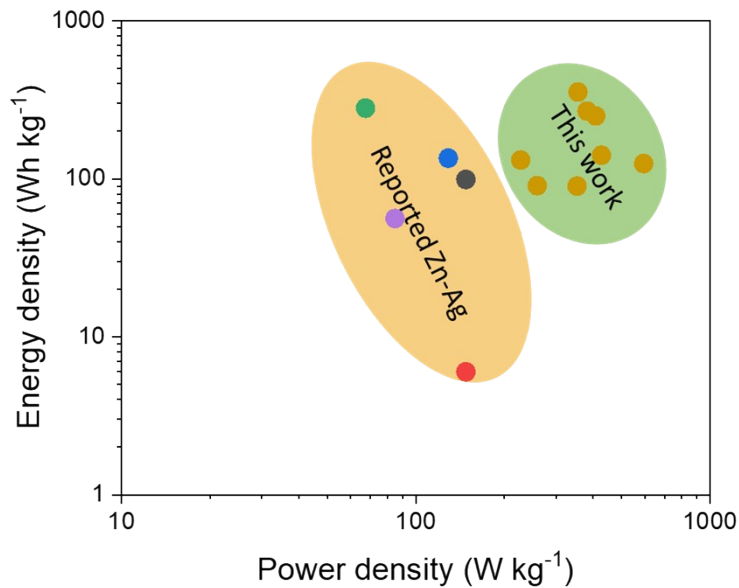
Fig. S3: Ragone plot for comparison of our work with previously reported Zn-Ag battery works.

3.2 Comparative Cyclic Voltammogram

A comparative cyclic voltammogram (CV) for both one and two e- redox suggests no additional peak in bimetallic nanostructures for gold redox reaction ($E^o_{Au^+/Au} = 2.12$ V vs Zn^{2+}/Zn) .
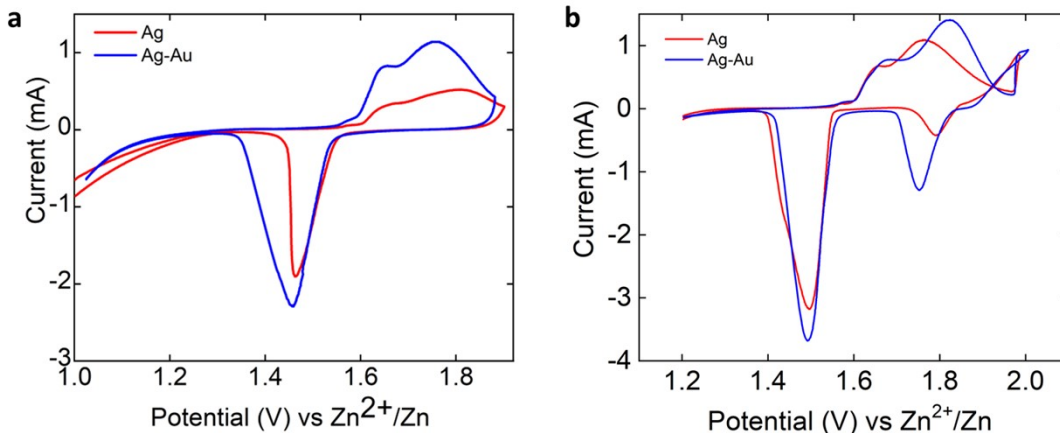

Fig. S4: Cyclic voltammograms (CV) of the Ag-Au nanostructures (blue) agrees with the CV of Ag (red) for two different potential windows **(a)** 1 V to 1.9 V vs Zn^{2+}/Zn and **(b)** 1.2 V to 2 V vs Zn^{2+}/Zn.

3.3 Electrochemical Impedance spectra

Electrochemical impedance spectroscopy was performed over a frequency range of 1 Hz to 100 kHz with an excitation voltage of 20 mV in a two-electrode geometry with as-prepared Ag-Au nanoparticles or Ag nanoparticles as the cathode. Zn foil is used as an anode for all measurements. All experimental EIS data was fitted using ZSimpWin software using a Randles equivalent circuit model, shown in the inset of main Fig.7a, for the Ag or Ag-Au electrode. Here, R_1 is approximated as solution resistance, R_2 is charge transfer resistance and Q_1 is the constant phase element which majorly comprises of the double layer capacitance. Q_2 is the constant phase element that captures the low frequency dynamics of the electrode. We measured the charge transfer resistance associated with Zn electrode to be relatively small ~3 Ω and insignificant compared to the contributions from the Au-Ag or Ag electrode. Hence, R_{ct} for Zn electrode has been neglected while fitting the circuit model.
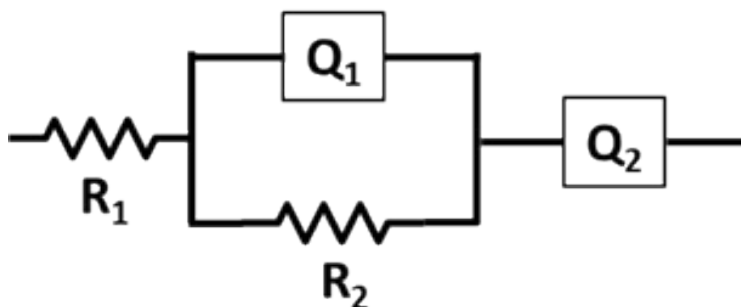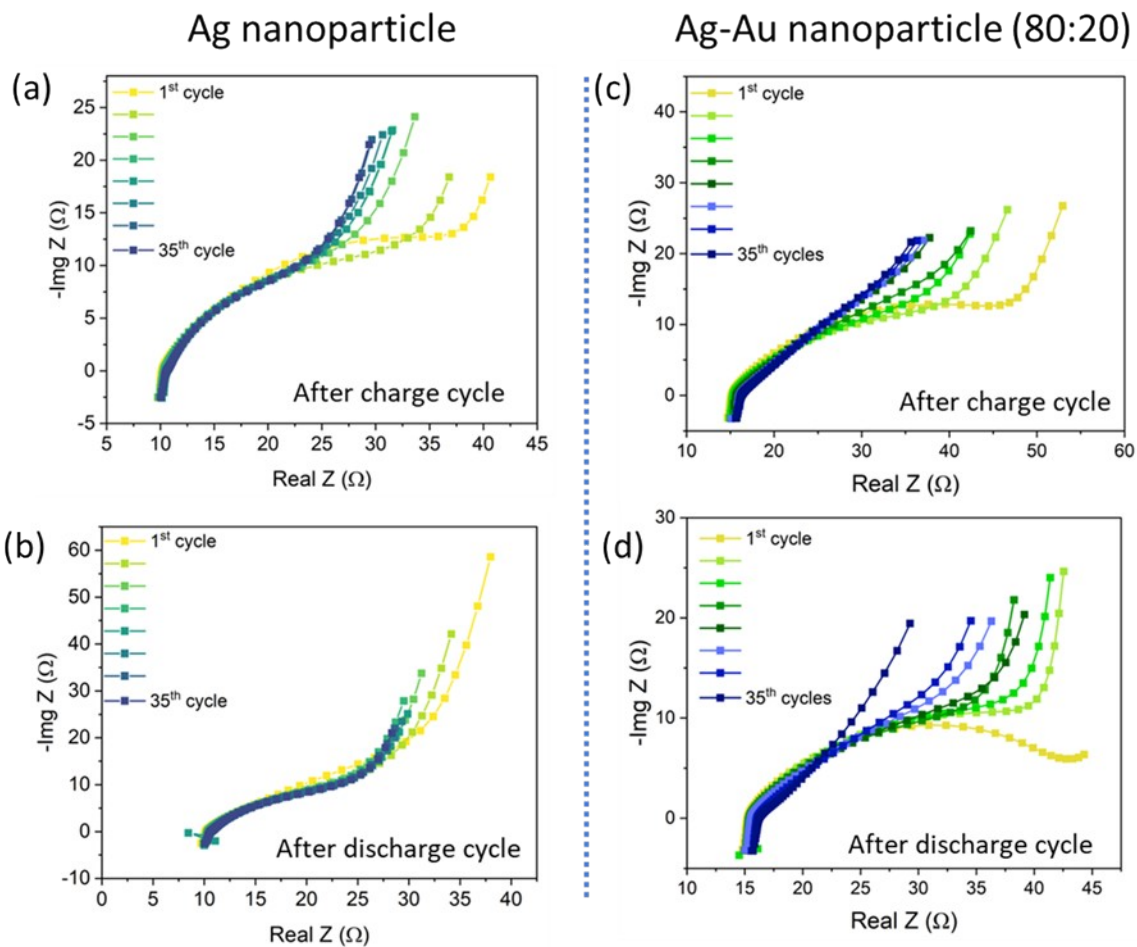
Fig. S5: A typical Nyquist plot for Zn-Ag battery after 1st charge cycle and then after 1st discharge cycle, and after every 5th charge and discharge cycles for both Ag nanostructures (**a** and **b**) and Ag-Au nanostructures (80:20 composition) for 2 e⁻ redox. (**c** and **d**).

3.4   Galvanostatic charge-discharge curves

GCD experiments for 80:20 and 70:30 Ag:Au compositions have been performed to identify the best performing composition under similar conditions mentioned above.
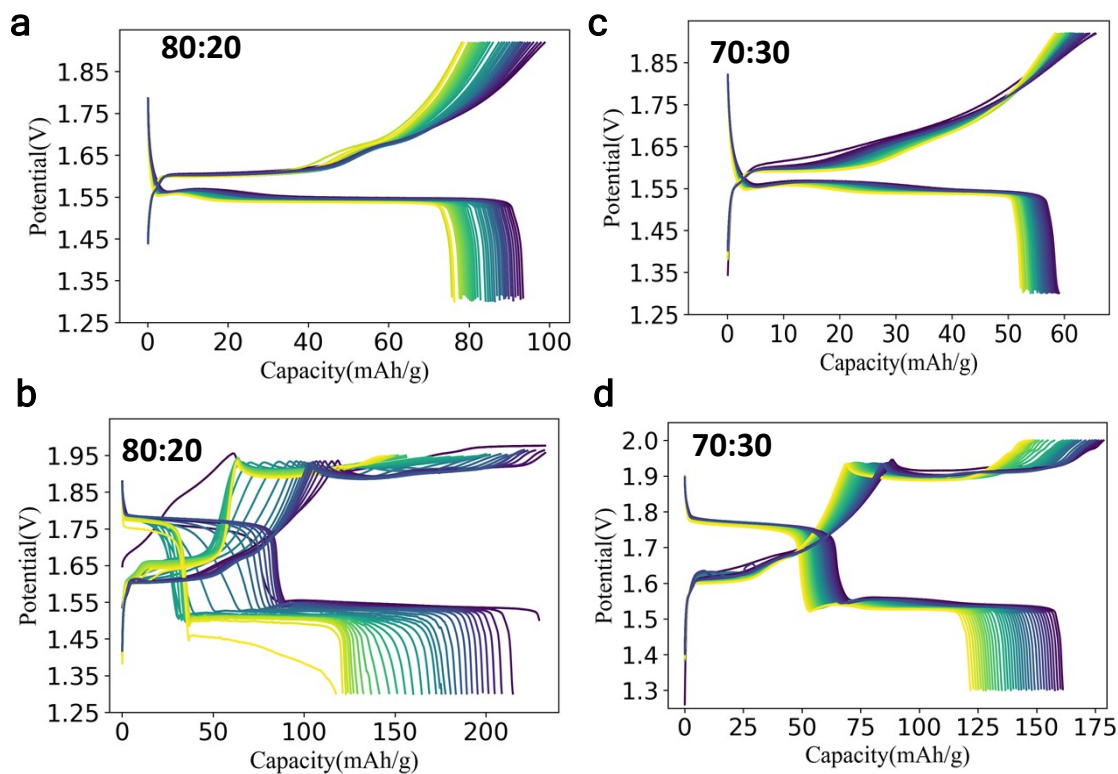
Fig. S6. Galvanostatic charge-discharge curves of Zn-Ag-Au battery with Ag:Au (80:20) (**a** and **b**) and for Ag:Au (70:30) (**c** and **d**) both for 1 e⁻ redox (**a, c**) and 2 e⁻ two redox (**b,d**).

4. Scanning Electron Microscopy-Energy Dispersive X-ray Spectroscopy (SEM-EDS)

SEM-EDS for pristine and cycled Ag and Ag:Au electrodes are performed to determine the elemental composition of Ag and Au using Ultra55 FE-SEM Karl Zeiss system, employing a high-efficiency secondary electron SE2 detector with accelerating voltage of 20 keV.

The table for the elemental composition for Ag and Au is presented in the table below.

Compositions of Ag and Au	Ratio of Ag and Au (Pristine)	Ratio of Ag and Au (1 e-redox)	Ratio of Ag and Au (2 e-redox)
Ag:Au – 90:10	8.54	6.55	1.4
Ag:Au – 80:20	3.8	1.25	0.45
Ag:Au – 70:30	2.1	2	1.9

Table S2: Comparison of the elemental composition of Ag and Au for pristine and cycled electrodes (both 1 and 2 e- transfer redox reactions).

5. References

[1] D. Ozgit, P. Hiralal and G. A. J. Amaratunga, *ACS Appl. Mater. Interfaces*, 2014, **6**, 20752–20757.

[2] A. Kota, L. W. Kum, K. Vallurupalli, A. Gogia, A. T. Neidhard-Doll and V. P. Chodavarapu, *Batteries*, 2022, **8**, 74.

[3] K. T. Braam, S. K. Volkman and V. Subramanian, Journal of Power Sources, 2012, **199**, 367–372.

[4] D. M. E. Garcia, A. S. T. M. Pereira, A. C. Almeida, U. S. Roma, A. B. A. Soler, P. D. Lacharmoise, I. M. Das Mercês Ferreira and C. C. D. Simão, *ACS Omega*, 2019, **4**, 16781–16788.

[5] C.-C. Chang, Y.-C. Lee, H.-J. Liao, Y.-T. Kao, J.-Y. An and D.-Y. Wang, *ACS Sustainable Chem. Eng.*, 2019, **7**, 2860–2866.